11164 *Inorg. Chem.* **2010**, *49*, 11164–11173
DOI: 10.1021/ic101756t

Inorganic Chemistry
Article

Adsorption and Separation of Organic Six-Membered Ring Analogues on Neutral Cd(II)-MOF Generated from Asymmetric Schiff-Base Ligand

Li Duan,[†] Zhen-Hua Wu,[†] Jian-Ping Ma,[†] Xiang-Wen Wu,[‡] and Yu-Bin Dong*,[†]

[†]*College of Chemistry, Chemical Engineering and Materials Science, Key Laboratory of Molecular and Nano Probes, Engineering Research Center of Pesticide and Medicine Intermediate Clean Production, Ministry of Education, Shandong Provincial Key Laboratory of Clean Production of Fine Chemicals, Shandong Normal University, Jinan 250014, People's Republic of China, and* [‡]*State Key Lab of Crystal Materials, Shandong University, Jinan 250100, People's Republic of China*

Received September 1, 2010

A new **CdL_2**-MOF was synthesized based on an asymmetric Schiff-base ligand **LH**, which is obtained by condensation of 5-formyl-8-hydroxyquinoline and 3-pyridinecarboxylic acid hydrazide. A series of organic six-membered ring analogues, namely, 1,4-dioxane, cyclohexane, cyclohexene, benzene, cyclohexanone, and cyclohexanol, can be absorbed by the **CdL_2** porous framework in liquid-phase to generate **$G_n \subset CdL_2$** (n = 1 and 2) host−guest complexes. In addition, the **CdL_2** host framework displays different affinity for these six-membered ring substrates and can effectively separate them under mild conditions (i.e., 1, 4-dioxane > cyclohexane > cyclohexene and benzene > cyclohexanone > cyclohexanol). The empty **CdL_2** displays strong green-yellow emission. Furthermore, these host−guest systems show an interesting guest-driven luminescent emission, and the emission intensities of these guest-loaded complexes are effectively reduced.

Introduction

Metal−organic frameworks (MOFs), as an emerging class of porous materials, display various applications in gas storage, separation, catalysis, luminescence and drug release.[1] Rationally designed self-assembled metal−organic hosts with well-defined inner cavities indeed provide a new functional chemical phase, which leads to a promising application in adsorption and effective separation of organic substrates which have similar shape, polarity and size. Related reported examples of sorption and separation of organic molecules include selective binding of acyclic molecules (for example, acyclic RCN, RH, and ROH)[2] and aromatic molecules (for example, aromatics, alkyl-, and active group-substituted aromatics).[3] Despite the large number of MOF materials described in the literature, however, reports of MOFs on the separation of cyclic organic analogs are scarce, especially those that respond to a specific substrate in the presence of other different potential competitors under mild conditions. Compared to the traditional method, for example distillation, chromatography and crystallization,[4] the molecular separation by MOFs can be expediently performed under ambient conditions, so this alternative approach can effectively avoid the decomposition or side reactions of organic substrates unstable at elevated temperature. For example, liquid carbonyl compounds are inclined to condense under higher temperature, so their separation by distillation is generally performed under reduced pressure, and sometimes by cryogenic distillation.[5] On the other hand, it is generally very hard to separate the organic chemicals by distillation if their boiling points within a temperature interval less than 30 °C.

*To whom correspondence should be addressed. E-mail: yubindong@sdnu.edu.cn.

(1) (a) Moulton, B.; Zaworotko, M. J. *Chem. Rev.* **2001**, *101*, 1629. (b) Yaghi, O. M.; O'Keeffe, M.; Ockwig, N. W.; Chae, H. K.; Eddaoudi, M.; Kim, J. *Nature* **2003**, *423*, 706. (c) Kitagawa, S.; Kitaura, R.; Noro, S.-I. *Angew. Chem., Int. Ed.* **2004**, *43*, 2334. (d) Kubas, G. *Chem. Rev.* **2007**, *107*, 4152. (e) Pluth, M. D.; Bergman, R. G.; Raymond, K. N. *Acc. Chem. Rev.* **2009**, *42*, 1650. (f) Farha, O. K.; Hupp, J. T. *Acc. Chem. Rev.* **2010**, *43*, 1166. (g) Corma, A.; García, H.; Xamena, F. X. L. *Chem. Rev.* **2010**, *110*, 4606. (h) Binnemans, K. *Chem. Rev.* **2009**, *109*, 4283.

(2) (a) Das, M. C.; Bharadwaj, P. K. *J. Am. Chem. Soc.* **2009**, *131*, 10942. (b) Chen, B.; Liang, C.; Yang, J.; Contreras, D. S.; Clancy, Y. L.; Lobkovsky, E. B.; Yaghi, O. M.; Dai, S. *Angew. Chem., Int. Ed.* **2006**, *45*, 1390. (c) Pan, L.; Parker, B.; Huang, X.; Olson, D. H.; Lee, J.; Li, J. *J. Am. Chem. Soc.* **2006**, *128*, 4180. (d) Maes, M.; Alaerts, L.; Vermoortele, F.; Ameloot, R.; Couck, S.; Finsy, V.; Denayer, J. F. M.; De Vos, D. E. *J. Am. Chem. Soc.* **2010**, *132*, 2284.

(3) (a) Wang, X.; Liu, L.; Jacobson, A. J. *Angew. Chem., Int. Ed.* **2006**, *45*, 6499. (b) Alaerts, L.; Maes, M.; Giebeler, L.; Jacobs, P. A.; Martens, J. A.; Denayer, J. F. M.; Kirschhock, C. E. A.; De Vos, D. E. *J. Am. Chem. Soc.* **2008**, *130*, 14170. (c) Cychosz, K. A.; Wong-Foy, A. G.; Matzger, A. J. *J. Am. Chem. Soc.* **2008**, *130*, 6938. (d) Choi, E.-Y.; Park, K.; Yang, C.-M.; Kim, H.; Son, J.-H.; Lee, S. W.; Lee., Y. H.; Min., D.; Kwon, Y.-U. *Chem.—Eur. J.* **2004**, *10*, 5535. (e) Finsy, V.; Verelst, H.; Alaert, L.; De Vos, D.; Jacobs, P. A.; Baron, G. V.; Denayer, J. F. M. *J. Am. Chem. Soc.* **2008**, *130*, 7110.

(4) (a) Chow, F. K.; Grushka, E. *Anal. Chem.* **1977**, *49*, 1756. (b) Young, P. R.; McNair, H. M. *Anal. Chem.* **1975**, *47*, 756.

(5) Berg, L. U. S. Patent 5453167, 1995.

Published on Web 10/25/2010

We have been exploring discrete and polymeric porous MOFs, in which bent five-membered heterocycle-bridged ligands were chosen as the building blocks. Some of these MOFs do display interesting selective molecular adsorption and separation for specific classes of organic chemicals in liquid and vapor phases, for example, C_6-C_8 alkyl-substituted aromatics, heterocyclic analogues, and reactive group-attached heterocyclic isomers.[6] With respect to the separation of organic molecules of different size and shape, new MOFs containing different functionalized cavities must be synthesized and the study leading to them investigated to generate a sufficiently large database from which high separation efficiencies for specific classes of MOFs can be deduced.

In this contribution, reversible adsorption and effective separation of a series of sixed-membered organic analogues, namely 1, 4-dioxane, cyclohexane, cyclohexene, benzene, cyclohexanone and cyclohexanol, is investigated based on a new Cd(II)-MOF generated from a new hydrazone Schiff-base ligand. Furthermore, guest encapsulated host−guest systems show an interesting guest-driven luminescent emission[7] in the solid state and they might have applications as a sensor for organic molecules.

Materials and Methods. $Cd(OAc)_2$ (Acros) was used as obtained without further purification. Infrared (IR) samples were prepared as KBr pellets, and spectra were obtained in the 400−4000 cm^{-1} range using a Perkin-Elmer 1600 FTIR spectrometer. Elemental analyses were performed on a Perkin-Elmer Model 2400 analyzer. ^1H NMR data were collected using an AM-300 spectrometer. Chemical shifts are reported in δ relative to TMS. All fluorescence measurements were carried out on a Cary Eclipse Spectrofluorimeter (Varian, Australia) equipped with a xenon lamp and quartz carrier at room temperature. Thermogravimetric analyses were carried out using a TA Instrument SDT 2960 simultaneous DTA-TGA under flowing nitrogen at a heating rate of 10 °C/min. XRD pattern were obtained on a D8 ADVANCE X-ray powder diffractometer (XRD) with CuKa radiation (λ = 1.5405 Å).

Results and Discussion

Ligand. The hydrazone Schiff-base ligand **LH** was expediently prepared in 86% yield by the Schiff-base condensation of 5-formyl-8-hydroxyquinoline and 3-pyridinecarboxylic acid hydrazide in the presence of HCOOH in ethanol at reflux. As shown in Scheme 1, **LH** is an unsymmetric ligand that contains two different terminal coordinating sites, that is, pyridyl and 8-hydroxyquinoline chelator. The 8-hydroxyquinoline chelator contains

Scheme 1. Synthesis of **L**

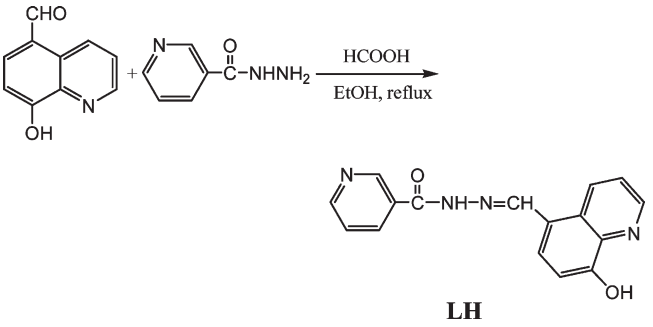

LH

Scheme 2. Synthesis of **1**−**6**

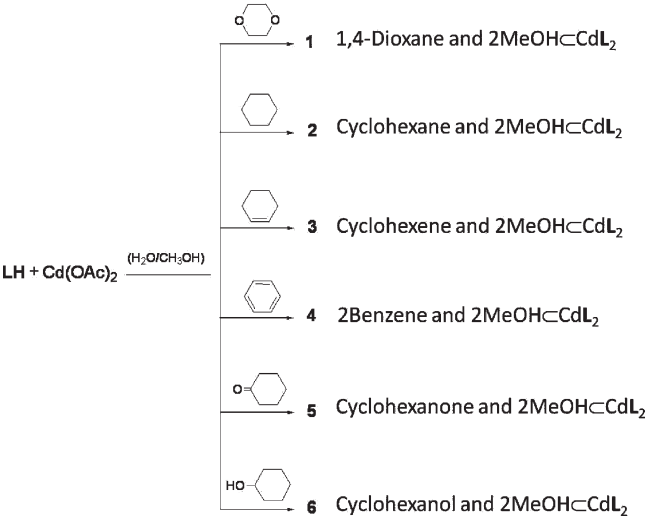

the N/O bidentate chelating motif that is usually binds the metal ions in a deprotonated way.[8] Upon deprotonation of its phenolic group, the ligand can form 2:1 complexes with M(II) ions in such a way that the resulting ML_2 species are neutral. So the combination of the divergent deprotonated **L** with octahedral coordinated M(II) cations herein would result in the neutral polymeric complexes. Compared to cationic MOFs, the neutral metal−organic frameworks are preponderant because they can save more vacant space, usually occupied by the counterions. In addition, **LH** is soluble in common polar organic solvents such as CH_2Cl_2, $CHCl_3$, THF, MeOH, and so on, which facilitates the reactions between it and metal ions in solutions.

Complexes Synthesis. The porous Cd(II)-MOF used as a selective absorbent was prepared by treating **L** with $Cd(OAc)_2 \cdot 6H_2O$ in a H_2O/MeOH/G (G = 1,4-dioxane (**1**), cyclohexane (**2**), cyclohexene (**3**), benzene (**4**), cyclohexanone (**5**), and cyclohexanol (**6**)) mixed solvent system at room temperature (Scheme 2). Yellow single crystals with a composition of $[CdL_2] \cdot (G_n) \cdot 2MeOH$ (G = 1,4-dioxane, n = 1 (**1**); cyclohexane, n = 1 (**2**); cyclohexene, n = 1 (**3**); benzene, n = 2 (**4**); cyclohexanone, n = 1 (**5**); and cyclohexanol, n = 1 (**6**)) were isolated in good yields. The X-ray crystal structure analysis revealed that compounds

(6) (a) Liu, Q.-K.; Ma, J.-P.; Dong, Y.-B. *J. Am. Chem. Soc.* **2010**, *132*, 7005. (b) Liu, Q.-K.; Ma, J.-P.; Dong, Y.-B. *Chem.—Eur. J.* **2009**, *15*, 10364. (c) Hou, G.-G.; Ma, J.-P.; Sun, T.; Dong, Y.-B.; Huang, R.-Q. *Chem.—Eur. J.* **2009**, *15*, 2261. (d) Dong, Y.-B.; Zhang, Q.; Wang, L.; Ma, J.-P.; Huang, R.-Q.; Shen, D.-Z.; Chen, D.-Z. *Inorg. Chem.* **2005**, *44*, 6591.

(7) (a) Lee, E. Y.; Jang, S. Y.; Suh, M. P. *J. Am. Chem. Soc.* **2005**, *127*, 6374. (b) Dong, Y.-B.; Wang, P.; Ma, J.-P.; Zhao, X.-X.; Wang, H.-Y.; Tang, B.; Huang, R.-Q. *J. Am. Chem. Soc.* **2007**, *129*, 4872. (c) Wang, P.; Ma, J.-P.; Dong, Y.-B.; Huang, R.-Q. *J. Am. Chem. Soc.* **2007**, *129*, 10620. (d) Bauer, C. A.; Timofeeva, T. V.; Settersten, T. B.; Patterson, B. D.; Liu, V. H.; Simmons, B. A.; Allendorf, M. D. *J. Am. Chem. Soc.* **2007**, *129*, 7136. (e) Wang, P.; Ma, J.-P.; Dong, Y.-B. *Chem.—Eur. J.* **2009**, *15*, 10432. (f) Liu, Q.-K.; Ma, J.-P.; Dong, Y.-B. *J. Am. Chem. Soc.* **2010**, *132*, 7005. (g) Stylianou, K. C.; Heck, R.; Chong, S. Y.; Bacsa, J.; Jones, J. T. A.; Khimyak, Y. Z.; Bradshaw, D.; Rosseinsky, M. J. *J. Am. Chem. Soc.* **2010**, *132*, 4119.

(8) (a) Palacios, M. A.; Wang, Z.; Montes, V. A.; Zyryanov, G. V.; A., P, Jr. *J. Am. Chem. Soc.* **2008**, *130*, 10307. (b) Vaira, M. D.; Bazzicalupi, C.; Orioli, P.; Messori, L.; Bruni, B.; Zatta, P. *Inorg. Chem.* **2004**, *43*, 3795.

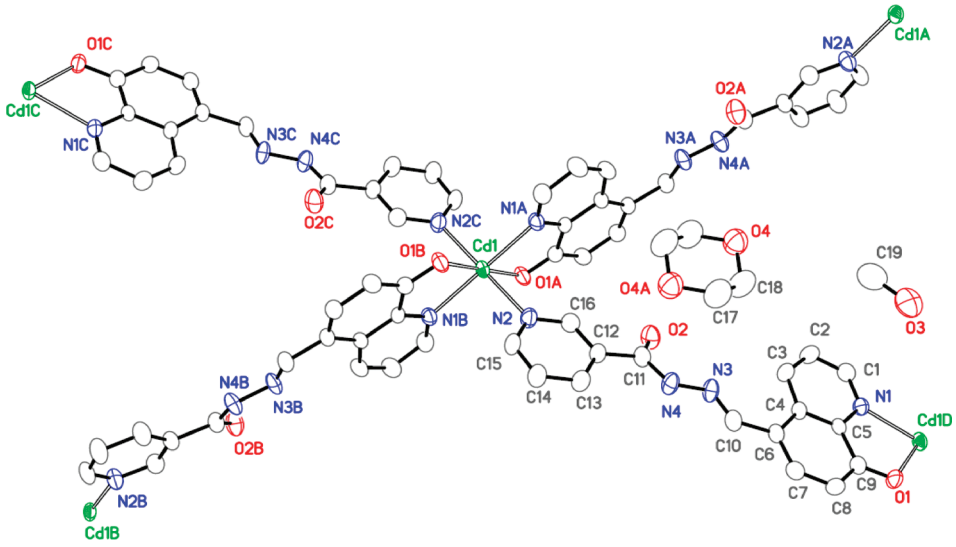

Figure 1. ORTEP figure of **1** (displacement ellipsoids drawn at 50% probability level).

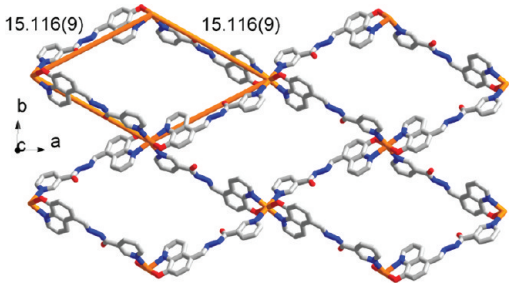

Figure 2. Two-dimensional net of **1** with an adjacent Cd···Cd separation of 15.116(9) Å.

1−**6** form isostructural two-dimensional coordination-driven networks $[\mathbf{CdL_2}]\cdot(\mathbf{G}_n)\cdot\mathbf{2MeOH}$ ($n = 1$ and 2), with corresponding guest molecules located in the channels formed by the stacking of these two-dimensional nets. Therefore, only the structure of **1** is described in detail herein.

As shown in Figure 1, the Cd(II) center in **1** displays a pseudo-octahedral coordination geometry. The octahedral sphere can be described as a basal plane associated with two hydroxyquinoline N/O chelators (N(1) and O(1)) from two **L** ligands (O(1)−Cd(1)−N(1) = 73.15(8)°), having Cd−O(1) and Cd−N(1) bond lengths of 2.261(2) and 2.309(2) Å, respectively, with axial positions occupied by two pyridyl N-donors N(2) (N(2)−Cd(1)−N(2) = 180.0°) with a Cd−N(2) bond distance of 2.420(3) Å. The octahedral Cd(II) nodes and **L** linkages build up a two-dimensional net consisting of parallelogram-like grids with a Cd···Cd distance of 15.116(9) Å (Figure 2). The nets are extended in the crystallographic *ab* plane and stack along the crystallographic [101] axis to generate rhombic channels. As indicated in Figure 3, the channel-frame is significantly reinforced by the Internet hydrogen bonding interactions ($d_{O(2)\cdots H(4)}$ = 2.07 Å, $d_{O(2)\cdots N(4)}$ = 2.912(4) Å, and ∠O(2)···H(4)−N(4) = 169°). The 1,4-dioxane and MeOH guests alternatively arrange in the channels and effectively take up the free space. In addition, the encapsulated MeOH molecules are hydrogen bonded to the phenolic oxygen ($d_{O(1)\cdots H(3A)}$ = 1.96 Å, $d_{O(1)\cdots O(3)}$ = 2.752(4) Å, and ∠O(1)···H(3A)−O(3) = 163.1°) on the framework, whereas the chair conformational 1, 4-dixoane molecules are suspended in the cavity (Figure 4).

The single-crystal structural analysis indicates that the framework of $\mathbf{CdL_2}$ herein does not show significant guest-dependent cell volume variation. The different guest species in **1**−**6** only result in a ∼5% cell variation (from 1812.1(5) to 1912.8(5) Å^3), which means the $\mathbf{CdL_2}$ framework is somewhat rigid. In other words, the presence of the different six-membered ring guests within the cavities has not a profound effect on the architecture of framework $\mathbf{CdL_2}$. The adjacent Cd···Cd distances of the two-dimensional nets in **2**−**6** are 15.139 (**2**), 15.138 (**3**), 15.154 (**4**), 15.209 (**5**), and 15.153 (**6**) Å, respectively. It is similar to **1**, all the encapsulated six-membered ring guests in **2**−**6** are suspended in the cavity, and no effective interhost−guest interactions are found. This could be the reason why the thermogravimeric analyses (TGA) for all six compounds show that the weight loss occurs at the very low temperature (Supporting Information). Notably, all two encapsulated MeOH molecules in **3**−**5** are hydrogen bonded to the framework through CH_3O−H···O-phenyl bonding linkages, while only one of two MeOH in **2** and **6** is hydrogen bonded to the framework (Figure 5). Cyclohexane, cyclohexanone and cyclohexanol guests in the cavities exist in a typical chair conformation, while cyclohexene molecule displays a half-chair conformation. Besides X-ray single crystal analysis, ^{1}H NMR spectra clearly indicate that the existence of the corresponding encapsulated six-membered ring guests and MeOH molecules, respectively (Figure 5).

Reversible Absorption. Compound **4** was chosen to performed the sorption experiment. Thermogravimeric analyses (TGA) together with ^{1}H NMR spectra indicate that all the benzene and MeOH guest molecules can be removed at 60−150 °C (Supporting Information). Notably, the suspended benzene guests can slowly escape from the framework at room temperature. The complete desolvated samples of **4a** were obtained by heating the crystals of **4** at 180 °C for about 30 min. The ^{1}H NMR spectrum of desolvated sample shows that the peaks corresponding to benzene (δ = 7.36 ppm) and MeOH (δ = 4.10 and 3.18 ppm) disappeared, which indicates the encapsulated guest

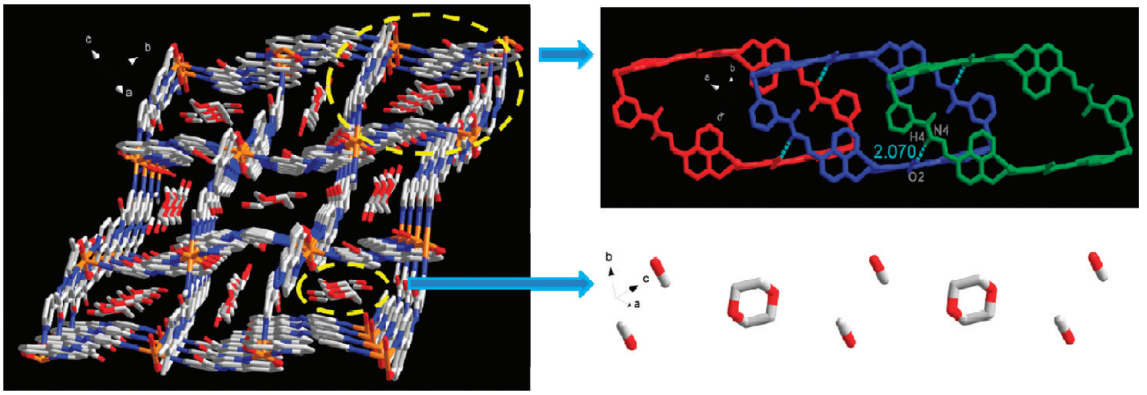

Figure 3. Two-dimensional nets of **1** are bound together through Internet hydrogen bonds to form a three-dimensional framework. The 1,4-dioxane and MeOH guests arrange alternatively in the channel.

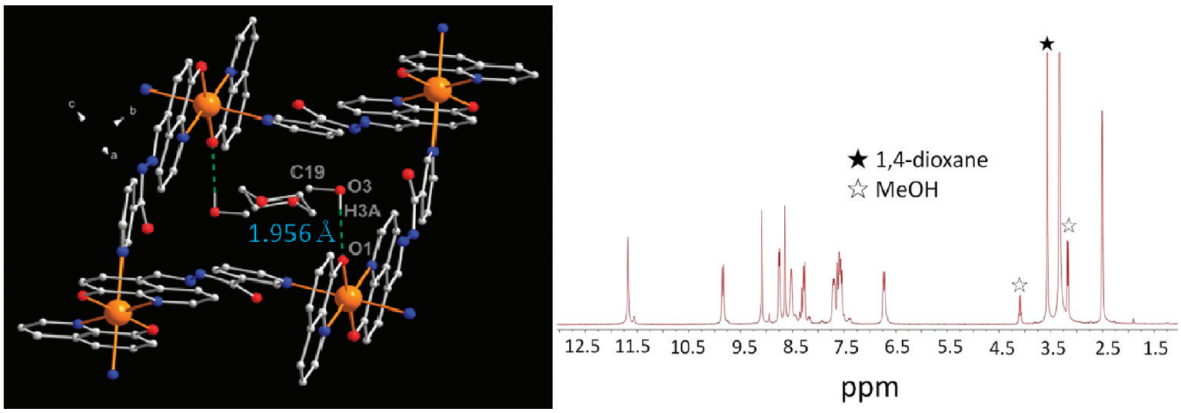

Figure 4. (a) MeOH guest are hydrogen bonded to the phenol on the framework, and no effective interactions between 1,4-dioxane and framework are found. (b) ^{1}H NMR (DMSO-d_6) spectrum of **1**. The marked signals correspond to the encapsulated 1,4-dixoane and MeOH, respectively.

molecules were completely removed to generate the corresponding empty framework of **4a**. The corresponding XRPD pattern of **4a** shows that the shapes and intensities of some reflections are slightly changed relative to that of the original sample (Figure 6). This means that guest loss does not result in symmetry change or cavity volume collapse. When the desolvated solids of **4a** are immersed in benzene for 48 h at room temperature, the single peak at 7.36 ppm appeared again in the ^{1}H NMR spectrum (no change after 48 h), clearly indicating benzene guest molecules were reincorporated into the framework (**4b**). Compared to **4**, the ^{1}H NMR spectrum indicates not all benzene guests recovered under experimental conditions, generating the host−guest system with a host/guest ratio of ~1:1.5. The XRPD pattern based on the regenerated sample of **4b** confirms that the **CdL$_2$** framework is stable during this reversible adsorption processes (Figure 6). Since **4** is insoluble in benzene, the possibility of a dissolution-recrystallization mechanism to explain the solvent reabsorption is unlikely.

Analogues Separation. All organic guests herein are six-membered ring, and most of them have similar molecular shape (conformation). On the other hand, some of them have very similar boiling points (Table 1). So their separation is a technical challenge. To explore the possibility of separating these six-membered ring organic analogies in liquid-phase, the desolvated sample of **4a** was immersed in a mixed-solvent system that consists of equimolar 1, 4-dioxane, cyclohexane, cyclohexene, benzene, cyclohexanone and cyclohexanol at room temperature for 10 h (no difference in binding was observed at the longer immersing times). The resulted sample was examined by ^{1}H NMR spectrum. The single peak at 3.56 ppm indicates that only 1, 4-dioxane was allowed into the pores of **CdL$_2$** to result in a new complex **1, 4-dioxane⊂CdL$_2$**, whereas no binding was observed for other five analogues by ^{1}H NMR (Figure 7). Such strong preference of **CdL$_2$** for 1, 4-dixoane suggests experimentally that these guest molecules are encapsulated inside the cavities instead of on the surface.[9] Furthermore, when the desolvated sample of **CdL$_2$** was immersed in a mixed solvent system of equimolar cyclohexane, cyclohexene, benzene, cyclohexanone and cyclohexanol at room temperature for 30 h (no change in binding was observed after 30 h, suggesting that the system researched an equilibrium by 30 h), only cyclohexane guest was taken inside (single peak at 1.39 ppm in ^{1}H NMR spectrum, Figure 8) to result in the formation of **cyclohexane⊂CdL$_2$**. The **CdL$_2$** framework is maintained upon selectivity, which is supported by the XRPD patterns (Figures 8). Therefore, among these six organic analogues (i.e., 1,4-dioxane, cyclohexane, cyclohexene, benzene, cyclohexanone, and cyclohexanol), 1,4-dioxane is the preferred guest for **CdL$_2$** over the rest five kinds of analogues. Among cyclohexane, cyclohexene, benzene,

(9) Dewal, M. B.; Lufaso, M. W.; Hughes, A. D.; Samuel, S. A.; Pellechia, P.; Shimizu, L. S. *Chem. Mater.* **2006**, *18*, 4855.

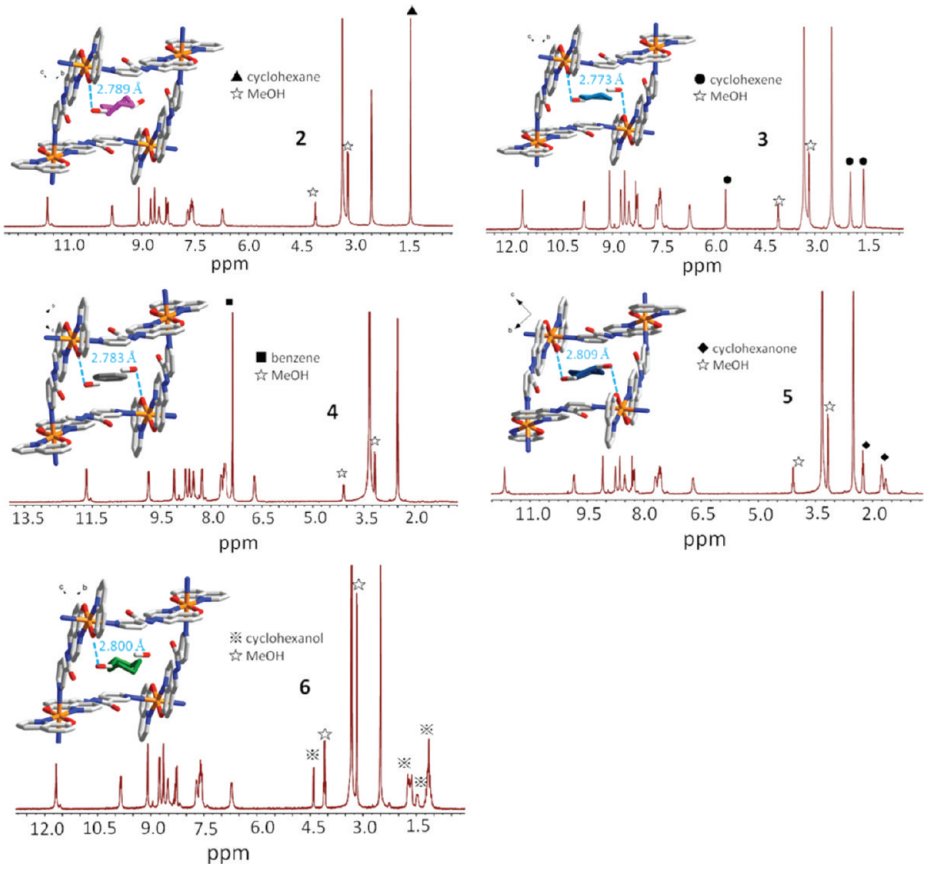

Figure 5. ^{1}H NMR spectra of **2**−**6** (DMSO-d_6). The ^{1}H NMR measurements were directly performed on the obtained single-crystals of **2**−**6** at room temperature in DMSO-d_6. MeOH, cyclohexane, cyclohexene, benzene, cyclohexanone and cyclohexanol proton peaks are marked, respectively. Single-crystal structures of **2**−**6** with corresponding encapsulated six-membered ring molecules and MeOH are inserted. The $CH_3O\cdots$O-phenyl distances are shown in the figures. X-ray single-crystal analysis indicates that the encapsulated cyclohexene (**3**), cyclohexanone (**5**), and cyclohexanol (**6**) guests are disordered to some extent in the cavities, so only major disordered components are shown in the figure.

cyclohexanone, and cyclohexanol, cyclohexane is preferred under the experimental conditions.

When the empty host of $\mathbf{CdL_2}$ was placed in a mixed-solvent of equimolar cyclohexene, benzene, cyclohexanone, and cyclohexanol for 120 h, and the $\mathbf{CdL_2}$ shows selective sorption of benzene (δ = 7.36 ppm) and cyclohexene (δ = 5.65, 2.50, and 1.55 ppm) to form benzene/cyclohexene⊂$\mathbf{CdL_2}$ with a ∼1:1 ratio, which is determined by the ^{1}H NMR spectrum (Figure 9). Again, the XRPD pattern indicates that the framework is stable during this process. However, the $\mathbf{CdL_2}$ cannot completely separate cyclohexanone and cyclohexanol under experimental conditions. The ^{1}H NMR spectrum performed on the sorption saturated sample obtained from a mixed cyclohexanone and cyclohexanol solvent indicates that both proton resonances corresponding to the cyclohexanone and cyclohexanol (about 2:1 ratio of cyclohexanone and cyclohexanol based on ^{1}H NMR spectrum) were observed (Figure 10). Thus, the separation of cyclohexanone and cyclohexanol by $\mathbf{CdL_2}$ is based mainly on preference instead of selectivity of target guest substrates.

It is well-known that the separation of cyclohexanol and cyclohexanone by distillation is very difficult because of their very similar boiling points (Table 1). Furthermore, cyclohexanone is inclined to condense at the temperature around its boiling point. As shown above, we cannot completely separate cyclohexanol and cyclohexanone directly on the empty $\mathbf{CdL_2}$ under experimental conditions. However, when crystallizes of $\mathbf{CdL_2}$ in a mixed solvent system MeOH/H_2O in the presence of equimolar cyclohexanone and cyclohexanol, only cyclohexanone and MeOH guest molecules other than cyclohexanol have been clathrated during the crystallization, which is clearly confirmed by its ^{1}H NMR spectrum (DMSO-d_6) (Figure 11). The selective encapsulation of $\mathbf{CdL_2}$ for cyclohexanone might be explained in terms of template-preference crystallization. Although cyclohexanol and cyclohexanone are similar in molecular shape and size, cyclohexanone is more polar (dielectric constants of 18.2 and 15.0 for cyclohexanone and cyclohexanol, respectively). It is likely that the −C(O)−NH−N=CH− bridging asymmetric ligand together with Cd(II) node form a polar interior around polar template preferentially. Such in situ separation of specific guest substrate from its competitors during crystallization process has been previously observed.[6d]

As shown above, the affinity order expressed by the $\mathbf{CdL_2}$ host for these guest molecules is 1,4-dioxane > cyclohexane > cyclohexene and benzene > cyclohexanone > cyclohexanol. So, herein, we might begin to rationalize the affinity and selectivity of guests binding in $\mathbf{CdL_2}$ mainly on the basis of their molecular conformation (i.e., molecular shape), polarity, and size. It seems that the chair conformational, polar and smaller organic substrates are preferentially adsorbed. The results herein might bear a practical relevance to the petroleum industry, such as in the separation of cyclohexane from benzene

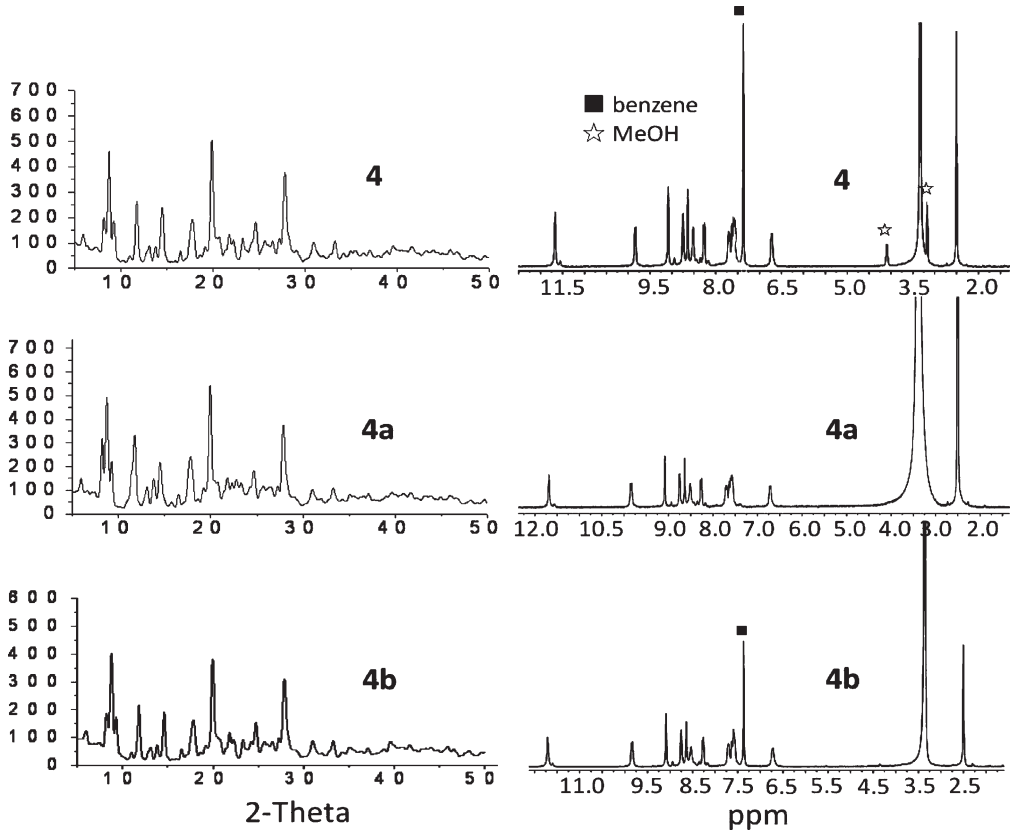

Figure 6. ^{1}H NMR spectra (DMSO-d_6) and corresponding XRPD patterns recorded at room temperature: (**4**) The as-synthesized sample of **4**. (**4a**) The solid sample of **4** was heated at 180 °C for 30 min. (**4b**) The desolvated solids **4a** immersed in benzene for 48 h and dried at room temperature for 48 h. The signals of benzene and MeOH molecules are marked, respectively.

Table 1. Guests' Boiling Points and Their Conformations in the Pores of CdL_2[a]

	1,4-dioxane	cyclohexane	cyclohexene	benzene	cyclohexanone	cyclohexanol
bp (°C)	101	81	83	80	155	162
shape	chair conformation	chair conformation	half-chair conformation	plane	chair conformation	chair conformation

[a] Guest molecular conformations were determined based on X-ray single-crystal diffraction.

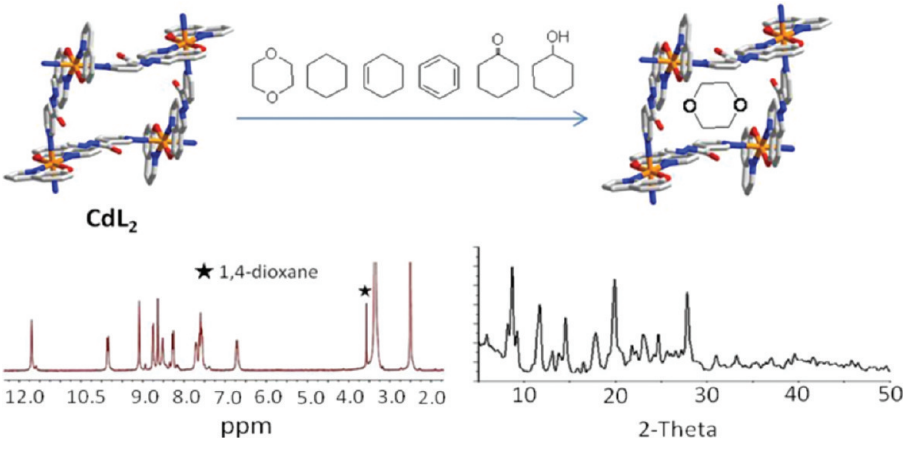

Figure 7. ^{1}H NMR spectrum (DMSO-d_6) and corresponding XRPD pattern obtained based on the desolvated sample immersed in a mixed-solvent system that consists of equimolar 1,4-dioxane, cyclohexane, cyclohexene, benzene, cyclohexanone, and cyclohexanol at room temperature for 10 h. The encapsulated 1,4-dioxane is marked.

and cyclohexene, and benzene from crude oil or gasoline. In addition, the separation of cyclohexanone from cyclohexane is very important in the production of nylons based on a cyclohexane oxidation approach.[10]

Guest-Driven Luminescence. MOFs have been investigated for fluorescence properties and for potential applications as

(10) Sun, H.; Blatter, F.; Frei, H. *J. Am. Chem. Soc.* **1996**, *118*, 6873.

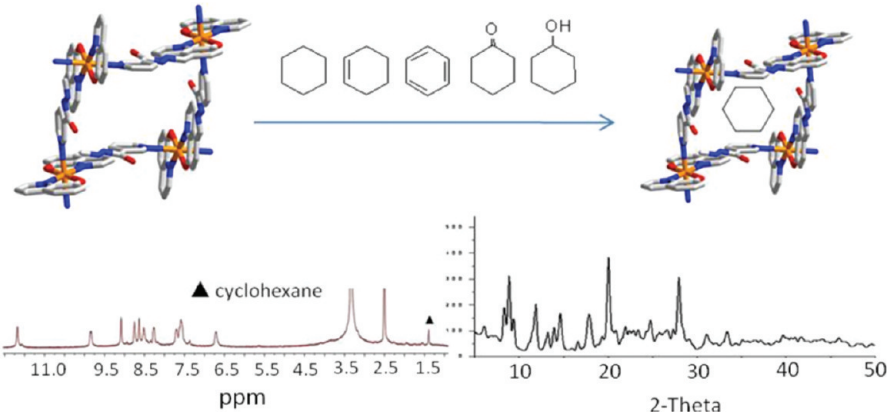

Figure 8. ^{1}H NMR spectrum (DMSO-d_6) and corresponding XRPD pattern obtained based on the desolvated sample immersed in a mixed-solvent system that consists of equimolar cyclohexane, cyclohexene, benzene, cyclohexanone, and cyclohexanol at room temperature for 30 h. The encapsulated cyclohexane is marked.

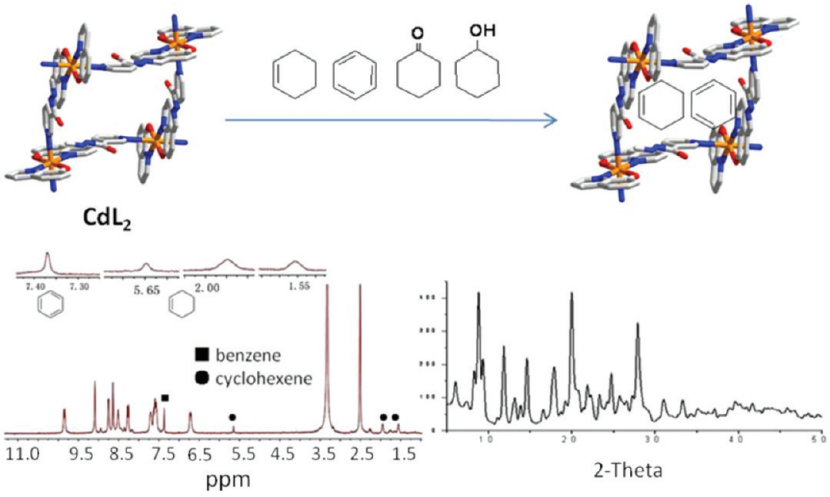

Figure 9. ^{1}H NMR spectrum (DMSO-d_6) and corresponding XRPD pattern obtained based on the desolvated sample immersed in a mixed-solvent system that consists of equimolar cyclohexene, benzene, cyclohexanone, and cyclohexanol at room temperature for 60 h. The encapsulated cyclohexene and benzene molecules are marked, respectively.

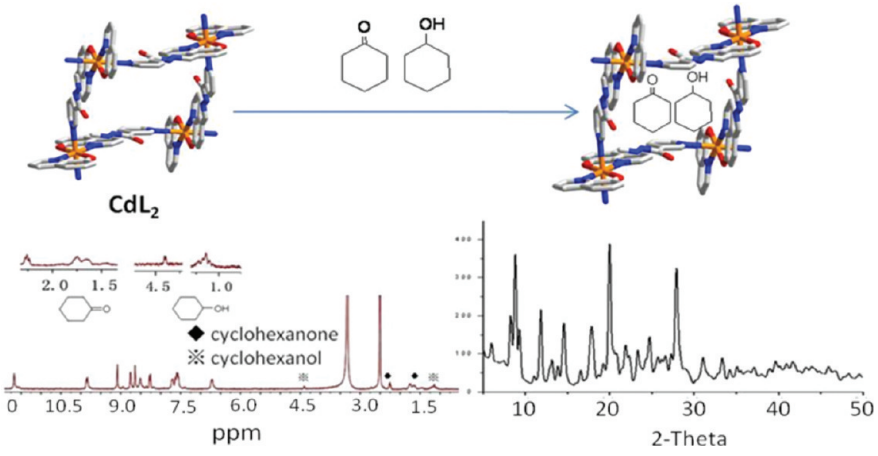

Figure 10. ^{1}H NMR spectrum (DMSO-d_6) and corresponding XRPD pattern obtained based on the desolvated sample immersed in a mixed-solvent system that consists of equimolar cyclohexanone and cyclohexanol at room temperature for 120 h. The encapsulated cyclohexanone and cyclohexanol molecules are marked, respectively.

luminescent materials.[11] Because of the higher thermal stability of inorganic−organic coordination polymers and the ability of affecting the emission wavelength of organic materials, syntheses of MOFs by the judicious choice of conjugated organic spacers and transition metal centers can be an efficient method for obtaining new types of electroluminescent materials, especially for d^{10} or d^{10}−d^{10} systems. Recently, we reported a series of

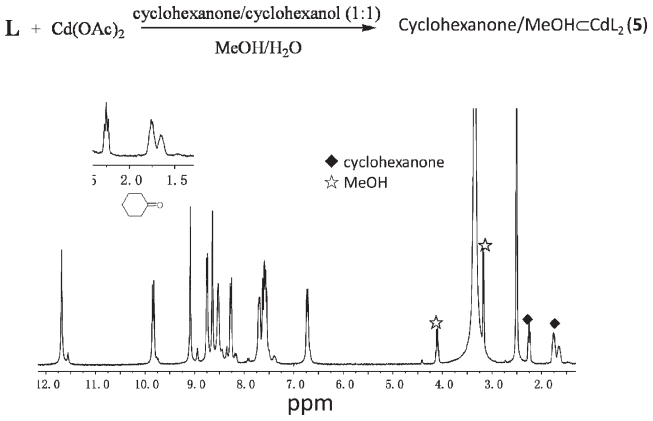

Figure 11. ^{1}H NMR spectrum (DMSO-d_6) of **cyclohexanone/MeOH⊂CdL$_2$** obtained from a mixed solvent system MeOH/H_2O in the presence of equimolar cyclohexanone and cyclohexanol. The encapsulated cyclohexanone and MeOH guest molecules are marked, respectively.

coordination-driven host−guest systems with interesting tunable luminescent property.[7a,b,d,e,12] The tunable luminescence (including tunable emission color[11a] and tunable emission intensity[7g]) is successfully realized by controlling the type of the encapsulated guest species.

To investigate the role of encapsulated guest in the emission property, emission spectra of empty **CdL$_2$** and the host−guest complexes of **1**−**6** were recorded in the solid state. As shown in Figure 12, desolvated **CdL$_2$** exhibits one emission maximum at 570 nm upon 467 nm excitation. In comparison with the emission for free **LH** (553 nm upon excitated at 448 nm, Supporting Information), the emission of desolvated **CdL$_2$** might be assigned to the ligand-centered (n−π* or π−π*) emission because similar emission bands are observed.[13] The slight difference in their emissions is probably because of the **L** coordination to metal ion in complex rather than to proton in **LH**.[13b] For **1**−**6**, the emission colors are in the range of 542−566 nm upon excitation at 467 nm (Figure 12), corresponding to the green-yellow colors, which are the most sensitive wavelengths for human eyes. The emission bands of guest-loaded **1**−**6** are slightly blue-shifted compared to the desolvated sample, which is clearly resulted from the loaded guest molecules. The emission intensities, however, are much reduced. Such emission quenching is distinct different from the host−guest systems of aromatics⊂**CdL$_2$** (aromatics = benzene, toluene, and *o*-, *m*-, *p*-xylene, L = 4-amino-3,5-bis(4-pyridyl-3-phenyl)-1,2,4-trizole) previously reported by us.[6b] Therein, the entry of aromatic hybrocarbons into **CdL$_2$** host leads to an ordered increase of the emission intensity as the guest size increases, which is contributed to the structural rigidity enhancement imposed by the host−guest interactions. The six-membered ring guests herein are suspensed in the cavities and not bound to the framework. So the observed emission quenching could be attributed to nonrediative energy transition. As shown in Figure 12, compound **4** exhibits the lowest emission intensity. As shown above, among compounds **1**−**6**, benzene guest binding in **4** is at the highest ratio (**CdL$_2$**/benzene = 1: 2). Logically, the more guest binding would lead to more nonrediative transition, consequently, the lower emission intensity.

Conclusion

In summary, six new host−guest supramolecular complexes **G$_n$⊂CdL$_2$** (G = 1,4-dioxane, cyclohexane, cyclohexene, benzene, cyclohexanone, and cyclohexanol, n = 1 and 2) have been synthesized based on a new asymmetric Schiff-base ligand **LH** and Cd(II) ion. Compounds **1**−**6** are isostructural and feature a two-dimensional net. These coordination-driven nets are linked together through interlayer hydrogen bonds to generate nanosized rhombic channels (~1.5 × 1.5 nm). Notably, the presence of the different six-membered ring templates within the cavities has not a profound effect on the architecture of framework **CdL$_2$**. In addition, the **CdL$_2$** host is robust and able to reversibly adsorb these six-membered ring analogues. More importantly, **CdL$_2$** displays a clear preference for these organic analogues (i.e., 1, 4-dioxane > cyclohexane > cyclohexene and benzene > cyclohexanone > cyclohexanol) on the basis of dimension, polarity and shape, and can effective separate them under mild conditions. In addition, the loaded **CdL$_2$** complexes exhibit guest-driven luminescence which might be applied as a sensor for organic molecules.

Experimental Section

Materials and Methods. Infrared spectroscopy (IR) samples were prepared as KBr pellets, and spectra were obtained in the 4000−400 cm^{-1} range using a Perkin-Elmer 1600 FTIR spectrometer. ^{1}H NMR data were collected using a AM-300 spectrometer. Chemical shifts are reported in δ relative to TMS. Element analyses were performed on a Perkin-Elmer model 240C analyzer. Fluorescence measurement were carried out on a cary Eclipse Spectrofluorimeter (Varian, Australia) equipped with a xenon lamp and quartz carrier at room temperature. ESR spectra were measured with a Bruker ESR300 spectrometer using quartz sample tube.

Synthesis of L. Nicotinic carboxhydrazide (155 mg, 1.24 mmol) and 5-formyl-8-hydroquinoline (215 mg, 1.24 mmol) were dissolved in EtOH (20 mL), followed by dropwise addition of two drops of formic acid. The mixture was refluxed for 8 h and filtered, and the resulting yellow crystalline solid was washed with hot EtOH two times and then dired in air (300 mg). Yield: 86%. mp: 252−255 °C. IR (KBr pellet cm^{-1}): 3331(s), 1638(vs), 1595(s), 1571(s), 1510(s), 1477(s), 1377(m), 1305(m), 1230(vs), 1198(s), 1148(s), 837(m), 705(s). ^{1}H NMR (300 MHz, $CDCl_3$, 25 °C, TMS, ppm): δ 11.98(s, 1H, −NH), 10.48(s, 1H, −OH), 9.61(s, 1H, $-C_5H_4N$), 9.09(s, 1H, −CH=N−), 8.94(d, 1H, $-C_5H_3N$), 8.76(d, 1H, $-C_5H_4N$), 8.36(d, 1H, $-C_5H_3N$), 8.29(d, 1H, $-C_5H_4N$), 7.97(d, 1H, $-C_6H_2$), 7.47(m, 2H, $-C_6H_2$, $-C_5H_3N$), 7.47(t, 1H, $-C_5H_4N$). Anal. Calcd for $C_{16}H_{12}N_4O_2$: C, 65.75; H, 4.14; N, 19.17. Found: C, 65.57; H, 4.05; N, 18.87.

Synthesis of 1. A solution of **L** (5.8 mg, 0.02 mmol) in MeOH/1,4-dioxane (8 mL, v/v = 4:1) was carefully layered onto an aqueous solution (8 mL) of $Cd(OAc)_2$ (13.8 mg,0.06 mmol). Diffusion between the two phases over a period of three days produced bright yellow crystals in 86% yield (7.84 mg, based on

(11) (a) McManus, G. J.; Perry, J. J., IV; Perry, M.; Wagner, B. D.; Zaworotko, M. J. *J. Am. Chem. Soc.* **2007**, *129*, 9094. (b) Chen, B.; Wang, L.; Zapata, F.; Qian, G.; Lobkovsky, E. B. *J. Am. Chem. Soc.* **2008**, *130*, 6718. (c) White, K. A.; Chengelis, D. A.; Gogick, K. A.; Stehman, J.; Rosi, N. L.; Petoud, S. *J. Am. Chem. Soc.* **2009**, *131*, 18069. (d) Ciurtin, D. M.; Pschirer, N. G.; Smith, M. D.; Bunz, U. H. F.; zur Loye, H.-C. *Chem. Mater.* **2001**, *13*, 2743.

(12) Wang, H.-Y.; Cheng, J.-Y.; Ma, J.-P.; Dong, Y.-B.; Huang, R.-Q. *Inorg. Chem.* **2010**, *49*, 2416.

(13) (a) Wang, S.-M.; Guo, S.-P.; Li, Y.; Cai, L.-Z.; Zou, J.-P.; Xu, G.; Zhou, W.-W.; Zheng, F.-K.; Guo, G.-C. *J. Am. Chem. Soc.* **2009**, *131*, 13572. (b) Fang, Q.; Zhu, G.; Xue, M.; Sun, J.; Sun, F.; Qiu, S. *Inorg. Chem.* **2006**, *45*, 3582.

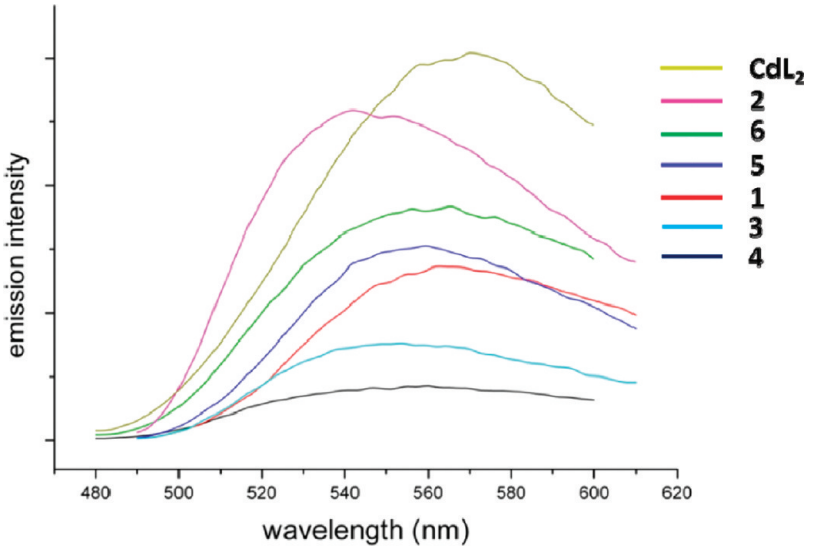

Figure 12. Solid-state luminescent spectra of desolvated CdL_2 (λ_{max} = 570 nm), **1** (λ_{max} = 563 nm), **2** (λ_{max} = 542 nm), **3** (λ_{max} = 553 nm), **4** (λ_{max} = 560 nm), **5** (λ_{max} = 559 nm), and **6** (λ_{max} = 566 nm) upon excitation at 467 nm.

L). IR (KBr pellet, cm^{-1}): 3421(m), 1637(vs), 1599(s), 1490(s), 1420(m), 1270(vs), 1210(s), 1163(s), 1075(s), 1016(m), 840(m), 755(m), 732(m), 679(m), 550(m). ^{1}H NMR (300 MHz, DMSO, 25 °C, TMS, ppm): δ 11.67(s, 1H, −NH−), 9.85(d,1H, $-C_9H_5N$), 9.09(s, 1H, $-C_5H_4N$), 8.76(d, 1H, $-C_5H_4N$), 8.64(s, 1H, −CH═N), 8.52(d, 2H, $-C_9H_5N$), 8.28(d, 1H, $-C_5H_4N$), 7.70(m, 2H, $-C_9H_5N$), 7.62(t, 1H, $-C_5H_4N$), 6.73(d, 1H, $-C_9H_5N$), 3.57(s, 8H, $-C_4H_8O$), 4.10(m, 1H, −OH), 3.18(d, 3H, $-CH_3$). Anal. Calcd for $C_{38}H_{38}N_8O_8Cd$: C, 53.87; H, 4.52; N, 13.23. Found: C, 53.85; H, 4.46; N, 13.00.

Synthesis of 2. Compound **2** was prepared by following the procedure described for **1** except by using cyclohexane instead of 1,4-dioxane to afford **2** (6.56 mg) as yellow crystal (yield, 78%, based on **L**). IR (KBr pellet, cm^{-1}): 3242(m), 1651(vs), 1589(s), 1550(s), 1463(m), 1270(vs), 1254(s), 1099(s), 1031(s), 964(m), 840(m), 755(m), 732(m), 679(m), 550(m). ^{1}H NMR (300 MHz, DMSO, 25 °C, TMS, ppm): δ 11.67(s, 1H, −NH−), 9.86(d, 1H, $-C_9H_5N$), 9.09(s, 1H, $-C_5H_4N$), 8.75(d, 1H, $-C_5H_4N$), 8.64(s, 1H, −CH═N), 8.50(d, 2H, $-C_9H_5N$), 8.28 (d, 1H, $-C_5H_4N$), 7.70(m, 2H, $-C_9H_5N$), 7.60(t, 1H, $-C_5H_4N$), 6.70(d, 1H, $-C_9H_5N$), 4.10(m, 1H, −OH), 3.18(d,3 H, $-CH_3$), 1.40(s, 12H, $-C_6H_{12}$). Anal. Calcd for $C_{40}H_{42}CdN_8O_6$: C, 56.92; H, 4.98; N, 13.28. Found: C, 57.01; H, 4.43; N, 13.15.

Synthesis of 3. Compound **3** was prepared by following the procedure described for **1** except by using cyclohexene instead of 1,4-dioxane to afford **3** (7.46 mg) as yellow crystal (yield, 76%, based on **L**). IR (KBr pellet, cm^{-1}): 3224(m), 1642(vs), 1590(s), 1551(s), 1420(m), 1270(vs), 1210(s), 1163(s), 1075(s), 1016(m), 840(m), 755(m), 732(m), 679(m), 489(m). ^{1}H NMR (300 MHz, DMSO, 25 °C, TMS, ppm): δ 11.67(s, 1H, −NH−), 9.86(d,1H, $-C_9H_5N$), 9.09(s, 1H, $-C_5H_4N$), 8.76(d, 1H, $-C_5H_4N$), 8.64(s, 1H, −CH═N), 8.51(d, 2H, $-C_9H_5N$), 8.28(d, 1H, $-C_5H_4N$), 7.70(m, 2H, $-C_9H_5N$), 7.60(t, 1H, $-C_5H_4N$), 6.70(d, 1H, $-C_9H_5N$), 5.65(m, 2H, −CH═CH−), 4.10(m, 1H, −OH), 3.18(d, 3H, $-CH_3$),1.95(m, 4H, $-CH_2$), 1.56(m,4H, $-CH_2$). Anal. Calcd for $C_{40}H_{40}CdN_8O_6$: C, 57.06; H, 4.76; N, 13.31. Found: C, 56.67; H, 4.45; N, 13.12.

Synthesis of 4. Compound **4** was prepared by following the procedure described for **1** except by using benzene instead of 1,4-dioxane to afford **4** (7.08 mg) as yellow crystal (yield, 78%, based on **L**). IR (KBr pellet, cm^{-1}): 3394(m), 1638(vs), 1610(s), 1490(s), 1420(m), 1270(vs), 1210(s), 1163(s), 1075(s), 1016(m), 840(m), 755(m), 732(m), 672(m), 511(m). ^{1}H NMR (300 MHz, DMSO, 25 °C, TMS, ppm): δ 11.67(s, 1H, −NH−), 9.86(d,1H, $-C_9H_5N$), 9.09(s, 1H, $-C_5H_4N$), 8.76(d, 1H, $-C_5H_4N$), 8.64(s, 1H, −CH═N), 8.52(d, 2H, $-C_9H_5N$), 8.28(d, 1H, $-C_5H_4N$), 7.70(m, 2H, $-C_9H_5N$), 7.60(t, 1H, $-C_5H_4N$), 7.36(s, 6H, C_6H_6), 6.73(d, 1H, $-C_9H_5N$), 4.10(m, 1H, −OH), 3.18(d, 3H, $-CH_3$). Anal. Calcd for $C_{40}H_{36}CdN_8O_6$: C, 57.34; H, 4.30; N, 13.38. Found: C, 57.16; H, 4.26; N, 13.18.

Synthesis of 5. Compound **5** was prepared by following the procedure described for **1** except by using cyclohexanone instead of 1,4-dioxane to afford **5** (7.46 mg) as yellow crystal (yield, 81%, based on **L**). IR (KBr pellet, cm^{-1}): 3421(m), 1703(vs), 1648(s), 1589(s), 1550(m), 1270(vs), 1462(s), 1163(s), 1075(s), 1016(m), 840(m), 755(m), 732(m), 679(m), 550(m). ^{1}H NMR (300 MHz, DMSO, 25 °C, TMS, ppm): δ 11.67 (s, 1H, −NH−), 9.86 (d, 1H, $-C_9H_5N$), 9.09 (s, 1H, $-C_5H_4N$), 8.76 (d, 1H, $-C_5H_4N$), 8.64 (s, 1H, −CH═N), 8.51 (d, 2H, $-C_9H_5N$), 8.28 (d, 1H, $-C_5H_4N$), 7.69 (m, 2H, $-C_9H_5N$), 7.59 (t, 1H, $-C_5H_4N$), 6.73 (d, 1H, $-C_9H_5N$), 4.10 (m, 1H, −OH), 3.18 (d, 3H, $-CH_3$), 2.27 (t, 4H, $-C_6H_{10}O$), 1.76 (m,4H, $-C_6H_{10}O$),1.64 (m, 2H, $-C_6H_{10}O$). Anal. Calcd for $C_{40}H_{40}CdN_8O_7$: C, 56.00; H, 4.67; N, 13.07. Found: C, 55.87; H, 4.65; N, 11.79.

Synthesis of 6. Compound **6** was prepared by following the procedure described for **1** except by using cyclohexanol instead of 1,4-dioxane to afford **6** (6.44 mg) as yellow crystal (yield, 75%, based on **L**). IR (KBr pellet, cm^{-1}): 3421(m), 1639(vs), 1551(s), 1507(s), 1460(m), 1395(vs), 1375(s), 1163(s), 1102(s), 1032(m), 840(m), 755(m), 732(m), 679(m), 550(m). ^{1}H NMR (300 MHz, DMSO, 25 °C, TMS, ppm): δ 11.67 (s, 1H, −NH−), 9.86 (d,1H, $-C_9H_5N$), 9.09 (s, 1H, $-C_5H_4N$), 8.75 (d, 1H, $-C_5H_4N$), 8.64 (s, 1H, −CH═N), 8.51(d, 2H, $-C_9H_5N$), 8.28 (d, 1H, $-C_5H_4N$), 7.70 (m, 2H, $-C_9H_5N$), 7.63 (t, 1H, $-C_5H_4N$), 6.73 (d, 1H, $-C_9H_5N$), 4.41 (m, 1H, $-C_6H_{12}O$), 4.11 (m, 1H, −OH,1H, $-C_6H_{12}O$)), 3.18 (d, 3H, $-CH_3$), 1.74 (t, 4, $-C_6H_{12}O$), 1.62(m, 2H, $-C_6H_{12}O$), 1.22(m, 4H, $-C_6H_{12}O$). Anal. Calcd for $C_{40}H_{42}CdN_8O_7$: C, 55.86; H, 4.89; N, 13.04. Found: C, 55.69; H, 4.57; N, 12.85.

Single-Crystal Structure Determination. Suitable single crystals of complexes were selected and mounted in air onto thin glass fibers. X-ray intensity data were measured at 298 K (for **1**, **4**, and **6**) and 173 K (for **2**, **3**, and **5**) on a Bruker SMART APEX CCD-based diffractometer (Mo Kα radiation, λ = 0.71073 Å). The raw frame data for the complexes were integrated into SHELX-format reflection files and corrected for Lorentz and polarization effects using SAINT.[14] Corrections for incident and diffracted beam absorption effects were applied using SADABS.[14] None of the

(14) *SADABS*; Bruker Analytical X-ray Systems, Inc.: Madison, WI, 1998.

Table 2. Crystal Data Collection and Structure Refinement for Compounds **1**−**6**

	1	**2**	**3**	**4**	**5**	**6**
empirical formula	$C_{38}H_{38}CdNO_8$	$C_{40}H_{42}CdN_8O_6$	$C_{40}H_{40}CdN_8O_6$	$C_{40}H_{36}CdN_8O_6$	$C_{40}H_{40}CdN_8O_7$	$C_{40}H_{42}CdN_8O_7$
fw	847.16	843.22	841.20	837.17	857.20	859.22
cryst syst	monoclinic	monoclinic	monoclinic	monoclinic	monoclinic	monoclinic
a (Å)	14.071(2)	14.065(2)	14.113(3)	14.097(3)	14.137(3)	14.071(2)
b (Å)	14.370(2)	14.593(2)	14.450(3)	14.255(3)	14.329(3)	14.775(2)
c (Å)	9.4824(15)	9.6737(14)	9.6194(18)	9.767(2)	9.662(2)	9.7851(15)
α (deg)	90	90	90	90	90	90
β (deg)	109.072(2)	109.441(2)	109.299(3)	108.617(3)	108.445(4)	109.908(2)
γ (deg)	90	90	90	90	90	90
V (Å^3)	1812.1(5)	1872.4(5)	1851.5(6)	1860.0(7)	1856.6(7)	1912.8(5)
space group	$P2_1/c$	$P2_1/c$	$P2_1/c$	$P2_1/c$	$P2_1/c$	$P2_1/c$
Z value	2	2	2	2	2	2
ρ calcd (g/cm^3)	1.553	1.492	1.509	1.495	1.533	1.492
μ(Mo Kα) (mm^{-1})	0.862	0.643	0.650	0.647	0.652	0.633
temp (K)	298(2)	173(2)	173(2)	298(2)	173(2)	298(2)
no. observations ($I > 3\sigma$)	3184	3303	3264	3275	3275	3370
final R indices [$I > 2\sigma(I)$]: R; R_w	0.0376, 0.0834	0.0425, 0.1203	0.0409, 0.0942	0.0312, 0.0757	0.0542, 0.1186	0.0503, 0.1377

crystals showed evidence of crystal decay during data collection. All structures were solved by a combination of direct methods and difference Fourier syntheses and refined against F^2 by the full-matrix least-squares technique. Non-hydrogen atoms were refined with anisotropic displacement parameters during the final cycles. Hydrogen atoms bonded to carbon and nitrogen were placed in geometrically idealized positions with isotropic displacement parameters set to 1.2 × U_{eq} of the attached atom. The oxygen-bonded hydrogen atoms were placed in geometrically idealized positions with isotropic displacement parameters set to 1.5Ueq of the attached atom. Crystal data, data collection parameters, and refinement statistics are listed in Table 2.

Acknowledgment. This work was supported by the National Natural Science Foundation of China (Grants 21072118 and 20871076), Shangdong Natural Science Foundation (Grant JQ200803), the Young Scientist Fund of Shandong Province of China (Grant 2007BS04002), and the Open Foundation of the State Key Laboratory of Crystal Materials of Shandong University (Grant KF0801).

Supporting Information Available: CIF files (**1**−**6**), interatomic distances and bond angles for **1**−**6**, TGA traces, and **LH** emission spectrum. This material is available free of charge via the Internet at http://pubs.acs.org.